A Segmentation-Based Multimodal Framework for Operational Landslide Mapping Using Post-Event SAR

R.G.C. Jeewantinie Kapilaratne[1*], Shin-Ichi Kaneta[1]

[1]Asia Air Survey Co. Ltd., 215-0004, Asaoku, Kawasaki, Kanagawa, Japan (jie.kapilaratne, sni.kaneta)@ajiko.co.jp

Keywords: Landslide Detection, Synthetic Aperture Radar (SAR), Multi-Source Geospatial Data, Red Relief Image Map (RRIM), Disaster Damage Assessment

Abstract

Rapid and reliable landslide mapping is critical for post-disaster response, yet Synthetic Aperture Radar (SAR)-based detection remains challenging due to speckle noise, geometric distortions, and complex terrain. This study develops an operational post-event landslide extraction framework using a UNet segmentation architecture with multimodal geospatial data fusion. High-resolution COSMO-SkyMed SAR imagery is combined with terrain representations derived from Digital Elevation Models (DEM), Red Relief Image Maps (RRIM), and rainfall indices to evaluate the contribution of complementary geospatial information to segmentation performance. Experiments were conducted across three major landslide-triggering events in Japan (Kyushu, Hokkaido, and Kumamoto), comparing SAR-only and multimodal configurations. Results demonstrate that integrating terrain information and rainfall data improves landslide detection performance compared with SAR-only inputs. RRIM consistently outperforms DEM as a topographic descriptor, particularly in steep or heterogeneous terrain, while rainfall information provides moderate gains in recall. Boundary-based metrics further indicate improved geometric fidelity of mapped landslides when multimodal inputs are incorporated. The framework requires only a single post-event SAR acquisition supplemented with publicly available ancillary datasets, enabling rapid and scalable generation of landslide inventories without reliance on pre-disaster imagery. These findings establish a reproducible baseline for SAR-driven landslide segmentation and highlight the potential of multimodal geospatial data fusion for operational disaster response and hazard monitoring.

1. Introduction

1.1 Landslide Mapping with SAR Data

Landslides are a major geohazard, causing severe economic losses, environmental degradation, and threats to human safety worldwide. Accurate and timely post-disaster landslide mapping underpins emergency response, susceptibility modelling, and long-term risk management. Conventional approaches, including field surveys and manual interpretation of optical satellite imagery, remain effective but are labour-intensive, time-consuming, and constrained by cloud cover and illumination conditions.

Synthetic Aperture Radar (SAR) imagery offers a robust alternative for rapid disaster mapping (Bovenga et al., 2012). Its day–night, all-weather observation capability and sensitivity to surface roughness and deformation make it particularly valuable for landslide detection in regions with frequent cloud cover. However, SAR interpretation is inherently challenging due to speckle noise, geometric distortions, and terrain heterogeneity, which together necessitate automated and scalable image analysis techniques (Barbera, 2014).

Most existing SAR-based landslide studies rely on change detection between pre-event and post-event images (e.g., coherence loss or intensity differencing) to identify newly triggered landslides (Bovenga et al., 2012). While effective, this approach depends on the availability of pre-event SAR scenes with consistent acquisition geometry and timing, which is often not feasible for rare or unexpected disasters. In contrast, this study focuses on post-disaster SAR imagery supplemented with ancillary geospatial data, eliminating the need for pre-event archives. This design enables rapid landslide mapping immediately after an event, even in regions where pre-disaster SAR data are unavailable, thereby enhancing the operational applicability of the approach.

This strategy is particularly relevant in the context of emerging SAR constellations (e.g., Capella, ICEYE, Umbra), which can deliver high-resolution and high-revisit imagery but frequently lack pre-event acquisitions with consistent geometry for every potential hazard location. By demonstrating that landslide delineation can be achieved using a single post-event SAR acquisition supplemented with ancillary geospatial datasets, this work provides a practical pathway for exploiting the growing volume of commercial and national SAR data streams for rapid hazard assessment.

Recent advances in deep learning have transformed remote sensing workflows. Convolutional Neural Networks (CNNs) and encoder–decoder architectures such as UNet (Ronneberger et al., 2015) can jointly capture global context and fine-grained spatial detail, enabling precise pixel-level classification. UNet, originally developed for biomedical segmentation, has proven especially effective for delineating landslide boundaries from remote sensing imagery.

Building on these developments, this study develops a UNet-based segmentation framework for landslide extraction from post-event SAR imagery and evaluates its performance across multiple landslide-triggering events. In addition to SAR observations, the framework incorporates complementary geospatial information including terrain representations derived from Digital Elevation Models (DEM), Red Relief Image Maps (RRIM), and rainfall indicators. By analysing the contribution of these modalities to landslide detection performance, the study aims to establish a robust baseline for multimodal landslide mapping using SAR data. The results provide insights into how terrain morphology and environmental conditions can enhance automated landslide detection and support the development of scalable AI-based workflows for rapid disaster response.

1.2 Related Work

Research in landslide detection has evolved significantly over the past two decades, progressing from manual interpretation to advanced machine learning and deep learning methods. This section reviews three relevant areas: (i) traditional and SAR-based landslide mapping, (ii) deep learning approaches for segmentation, and (iii) emerging multimodal fusion techniques.

This contribution has been peer-reviewed. The double-blind peer-review was conducted on the basis of the full paper.
https://doi.org/10.5194/isprs-annals-XI-3-2026-895-2026

1.2.1 Traditional and SAR-Based Landslide Mapping: Historically, landslide inventories have been generated using visual interpretation of optical satellite imagery or aerial photographs, often supported by field surveys (Guzzetti et al., 2012). While accurate, these approaches are resource-intensive and time-consuming, limiting their applicability for rapid disaster response. The emergence of Synthetic Aperture Radar (SAR) has addressed some of these challenges by providing day-and-night, all-weather imaging capabilities. SAR-based studies have applied intensity differencing, coherence change detection, and polarimetric decomposition to identify landslide-affected areas (Bovenga et al., 2012 and Mondini, 2017). However, SAR data interpretation remains non-trivial due to speckle noise, foreshortening, and layover effects in mountainous terrain. These limitations underscore the need for automated, scalable methods capable of extracting meaningful features from SAR imagery.

1.2.2 Deep Learning for Landslide Detection: Deep learning, particularly Convolutional Neural Networks (CNNs), has transformed remote sensing image analysis by enabling pixel-level classification and feature extraction. The UNet architecture (Ronneberger et al., 2015), originally designed for biomedical segmentation, has been widely adapted in geospatial applications due to its encoder–decoder design and skip connections, which capture both global context and fine-grained spatial details. In landslide mapping, CNN- and UNet-based methods have demonstrated improved accuracy over traditional classification techniques, effectively delineating landslide boundaries from optical imagery (Ghorbanzadeh et al., 2019) and SAR data (Liu et al., 2021). Despite these successes, many studies remain single modality, relying primarily on SAR or optical inputs, which may limit performance in regions with heterogeneous terrain or ambiguous backscatter signatures.

1.2.3 Emerging Multimodal Fusion Approaches: Recent advances in remote sensing research highlight the value of multimodal data fusion for improving classification robustness. By integrating complementary datasets such as SAR, optical imagery, Digital Elevation Models (DEM), and environmental indices multimodal models can capture both spectral and contextual features of geohazards (Zhang et al., 2024). Fusion techniques range from early fusion, where data layers are combined as multi-channel inputs, to late fusion approaches that merge model predictions. Transformer-based models and attention mechanisms have shown promise in dynamically weighting different modalities, enabling more reliable mapping of complex landscapes (Dosovitskiy et al., 2021; Hong et al., 2021).

While multimodal frameworks have been applied to land cover classification and disaster monitoring, their application to rapid landslide mapping remains limited. Most studies either rely on optical imagery, which is often unavailable in cloudy conditions, or lack large-scale operational workflows. This study contributes to bridging this gap by establishing a SAR-only UNet-based landslide detection framework as a baseline, with the goal of extending it into a multimodal AI system in future research.

2. Materials and Methods

2.1 Study Areas and Disaster Events

The study focuses on these three major landslide-triggering events in Japan as shown in Figure 1 and Table 1.

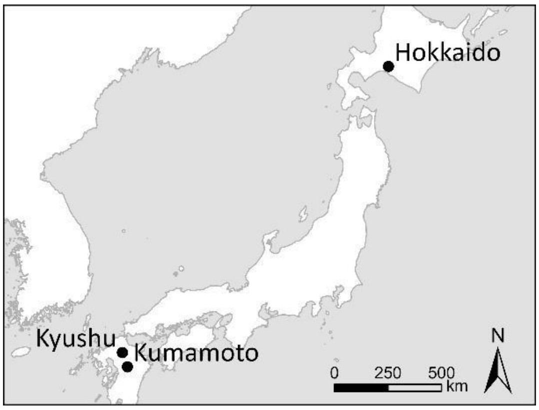

Figure 1. Locations of the three study areas (Kyushu, Hokkaido, Kumamoto) used for evaluating the proposed landslide detection framework.

These events represent distinct triggering mechanisms (rainfall- vs. earthquake-induced) and diverse topographic and land-use contexts, enabling robust model evaluation. For each event, the final ground-truth landslide inventories were compiled using publicly available landslide masks provided by the Geospatial Information Authority of Japan (GSI) and further verified using post-disaster optical satellite imagery. The datasets used for each study area are summarized in Table 1.

Table 1. Summary of Disaster Events and Corresponding COSMO-SkyMed Post-Event SAR and Optical Image Acquisition Dates Used in This Study.

Disaster Location	Disaster occurrence	CSK imaging date: orbital direction	Optical image observation Date
Kumamoto	16/04/2016	23/04/2016: A	29/04/2016
Kyushu	05~06/07/2017	18/07/2017: A	10/09/2017
Hokkaido	06/09/2018	08/09/2018: A	20/10/2018

2.2 Datasets

2.2.1 SAR Imagery: Post-event SAR data from **CSK (COSMO-SkyMed)** was used for all events. SAR images were radiometrically calibrated, co-registered, and resampled to a uniform spatial resolution (2.5 m). This imagery serves as the primary input and baseline for the study.

2.2.2 Relief Representations: Two elevation-derived products were evaluated as relief inputs:

Digital Elevation Model (DEM): from the Geospatial Information Authority of Japan (GSI).

Red Relief Image Map (RRIM): a derived relief visualization highlighting micro-topographic features (Chiba et al., 2008), produced from 10m resolution elevation data. This dual approach enables direct comparison between DEM and RRIM as relief sources.

https://doi.org/10.5194/isprs-annals-XI-3-2026-895-2026 | © Author(s) 2026. CC BY 4.0 License.

2.2.3 Rainfall Data

Rainfall data were incorporated to represent precipitation conditions associated with landslide-triggering events. Precipitation observations were obtained from the Automated Meteorological Data Acquisition System (AMeDAS) operated by the Japan Meteorological Agency (JMA). Weekly accumulated rainfall values corresponding to each event were calculated from nearby AMeDAS stations and used as auxiliary input to represent antecedent rainfall conditions.

2.3 UNet-Based Segmentation Framework

A UNet encoder–decoder architecture was implemented for pixel-wise landslide segmentation. The model accepts multi-source geospatial data as stacked input channels, enabling joint learning of spectral, topographic, and environmental features. The proposed framework is illustrated in Figure 2.

- **Encoder:** Convolutional layers with ReLU activation and max-pooling to extract hierarchical features.
- **Decoder:** Up-sampling layers with skip connections to recover fine spatial details and generate high-resolution segmentation outputs.

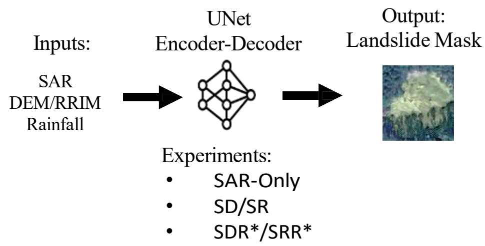

Figure 2. Overview of the proposed UNet-based multimodal landslide segmentation framework.

2.4 Experimental Design

To quantify the influence of each data source, five experimental configurations were designed: All experiments used the same UNet architecture, training protocol, and data splits**.** Differences in performance stem solely from the input data composition. This controlled setup enables direct evaluation of:

1. The improvement of multi-source input over SAR-only baseline.
2. The comparative effectiveness of DEM and RRIM as terrain representations.
3. The contribution of rainfall information when combined with SAR and terrain inputs.

The input configurations are summarized in Table 2.

2.5 Training and Evaluation Protocol

The model was trained using a supervised learning paradigm with annotated landslide masks serving as ground-truth labels. The dataset was divided into training (80%) and testing (20%) subsets, ensuring representative coverage of landslide and non-landslide regions across the study areas.

Table 2. Input Data Configuration Per Experiment

Experiment	SAR	DEM	RRIM	Rainfall*
SAR-Only (Baseline)	✓	–	–	–
SD	✓	✓	–	–
SR	✓	–	✓	–
SDR*	✓	✓	–	✓
SRR*	✓	–	✓	✓

Image tiles extracted from the SAR and auxiliary datasets were used as input samples for training. Data augmentation techniques, including random rotations, horizontal and vertical flips, and intensity normalization, were applied to mitigate overfitting and improve robustness to scene variations.

2.5.1 Evaluation Metrics:

To comprehensively evaluate model performance, three categories of metrics were adopted.

Conventional Pixel-Level Metrics: pixel-level agreement was quantified using common segmentation metrics Intersection over Union (IoU), F1-Score (Dice Coefficient) and Precision and Recall.

Boundary and Structure Metrics: Because accurate delineation of landslide boundaries is critical for post-disaster response and hazard assessment, additional metrics were used to evaluate boundary adherence and structural consistency.

Boundary F1 Score (BF1): Evaluates the alignment of predicted and reference boundaries within a specified tolerance. This study adopted 3 pixels (7.5m) tolerance for the BF1 estimation.
Cohen’s Kappa (κ): Measures agreement between prediction and reference while correcting for chance agreement (1).

$$\kappa = \frac{2[(TP*TN)]-(FN*FP)}{[(TP+FP)*(FP+TN)+(TP+FN)*(FN+TN)]} \tag{1}$$

where, TP: True positive TN: True negative
FN: False negative FP: False positive

Balanced Accuracy: Averaged sensitivity and specificity across classes (2).

$$Balanced\ Accuracy\ = \frac{Sensitivity\ +Specificity}{2} \tag{2}$$

where, Sensitivity = TP/(TP+FN) Specificity = TN/(TN+FP)

Together, these metrics provide a comprehensive assessment of segmentation performance by evaluating pixel-level accuracy, boundary precision, and structural consistency of the detected landslide polygons. This combination ensures fair and consistent comparison across all experimental configurations.

3. Results and Discussion

This section presents the model performance qualitatively (Figure 3, Figure 4) and quantitatively upon the ground truth landslide data.

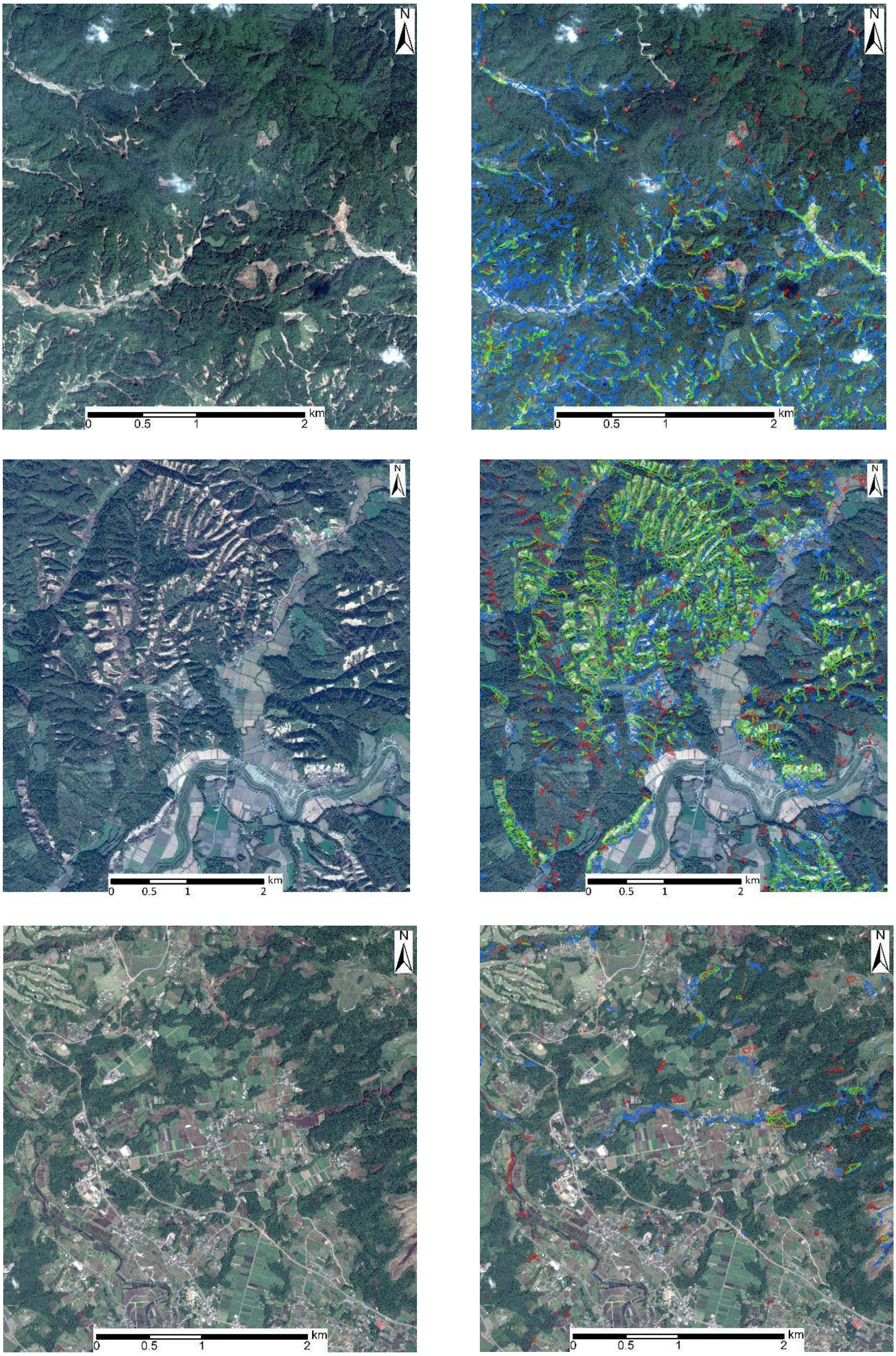

Figure 3. Qualitative comparison of predicted landslide masks with ground-truth annotations for representative samples from (a) Kyushu, (b) Hokkaido, and (c) Kumamoto, illustrating spatial variability in landslide characteristics across study regions.

True Positive False Positive False Negative

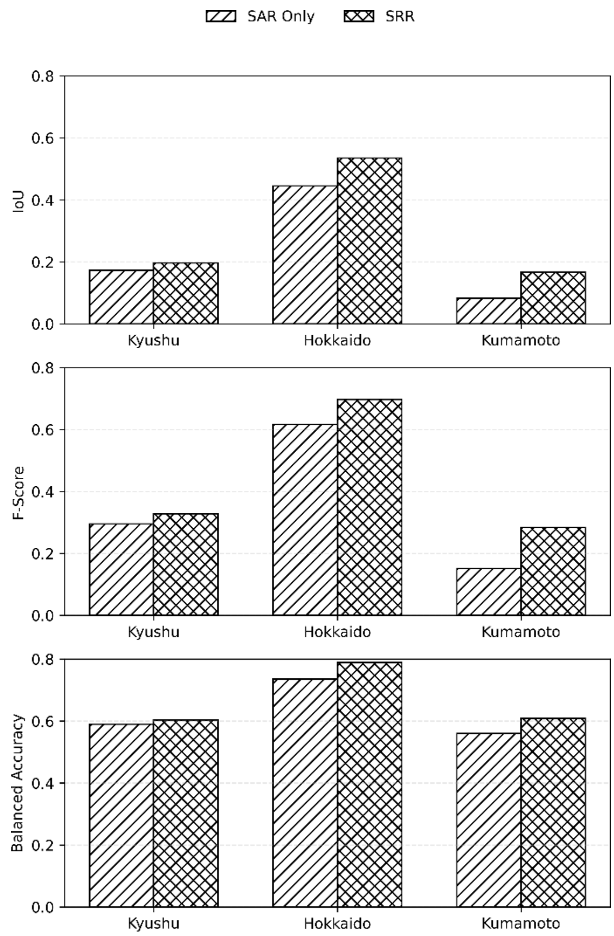

Figure 4. Site-specific performance metrics (IoU, F1-score, Kappa, Boundary F1, Balanced Accuracy) comparing SAR-only and multimodal configurations across Kyushu, Hokkaido, and Kumamoto.

3.1 Site-Specific Performance Across Case Studies

The segmentation performance varies substantially across the three study areas, indicating that landslide detection accuracy is strongly influenced by local terrain characteristics and landslide morphology. Table 3 summarizes the quantitative results for each site under different experimental configurations.

Among the three case studies, the Hokkaido Eastern Iburi earthquake area exhibits the highest overall performance. The SAR-only configuration already achieves an F-score of 0.616 and IoU of 0.445, indicating that the radar backscatter signal captures clear surface disturbances associated with the landslides. Incorporating terrain information and rainfall further improves the results, with the SRR configuration achieving the best performance (F-score = 0.697, IoU = 0.535). The improvements in Balanced Accuracy (0.736 → 0.789) and Cohen′s Kappa (0.549 → 0.637) suggest that additional geospatial inputs help the model better discriminate landslide areas from surrounding terrain. The relatively strong performance in Hokkaido can be attributed to the large and spatially continuous landslide scars produced by the 2018 earthquake, which generate clear geomorphological signatures that are effectively captured by both SAR backscatter and terrain representations.

In the Kyushu case study, the SAR-only configuration achieves a moderate F-score of 0.295 and IoU of 0.173. Incorporating terrain and rainfall information leads to modest but consistent improvements. The best configuration (SRR) increases the F-score to 0.328 while maintaining similar overall accuracy. Compared with Hokkaido, the improvements are smaller, likely due to the more heterogeneous terrain conditions and the presence of smaller and more fragmented landslides. In such environments, the radar signal may exhibit weaker contrast between landslide and non-landslide areas, making segmentation more challenging.

The Kumamoto earthquake case study presents the most challenging conditions for automated landslide mapping. Although the SAR-only model achieves high overall accuracy (0.98), the IoU (0.082) and F-score (0.151) remain very low due to the extreme class imbalance, as landslides occupy only a small proportion of the total study area. In this dataset, the number of landslide pixels is significantly smaller than in the other study areas, which limits the model's ability to learn representative landslide features and increases the likelihood of false negatives. Multi-source configurations improve the results, particularly when RRIM and rainfall are incorporated. The SRR configuration increases the F-score to 0.284 and IoU to 0.166, representing the largest relative improvement among the tested configurations. Nevertheless, the overall performance remains lower than in the other sites, reflecting the difficulty of detecting small and spatially dispersed landslides under conditions of severe class imbalance.

Overall, these site-specific results highlight that the effectiveness of the proposed framework depends strongly on landslide size, density, and terrain complexity. The model performs particularly well in environments where landslides form large, continuous scars with distinct geomorphological signatures, as observed in Hokkaido. In contrast, areas characterized by sparse or small landslides present greater challenges for segmentation models, even when additional geospatial information is incorporated.

3.2 Overall Performance Trends

Although segmentation performance varies across individual study areas, several consistent trends emerge across the experimental configurations. In general, incorporating additional geospatial inputs alongside SAR imagery improves landslide detection compared with the SAR-only baseline. Across all three case studies, configurations that integrate terrain representations and rainfall information tend to achieve higher F-scores, IoU values, and Cohen's Kappa than the SAR-only model.

The results indicate that terrain information plays a particularly important role in improving model performance. Configurations that include either DEM or RRIM consistently outperform the SAR-only baseline, suggesting that topographic context helps the model distinguish landslide features from surrounding terrain. Rainfall data further improves recall in several configurations, reflecting its value as an environmental indicator associated with landslide triggering conditions.

Despite these improvements, the magnitude of performance gains varies across the study areas, as discussed in Section 3.1. This variability highlights the influence of local

https://doi.org/10.5194/isprs-annals-XI-3-2026-895-2026

geomorphological conditions and landslide characteristics on segmentation performance. Nevertheless, the consistent improvements observed across multiple experimental configurations demonstrate the overall benefit of integrating complementary geospatial information with SAR imagery for automated landslide mapping.

Table 3. Site-wise Quantitative Performance of All Experimental Configurations Across Three Study Areas.

Exp. Name	IoU	F1-score	Cohen’s Kappa	Balanced Accuracy	Boundary F1-score
Kyushu					
SAR-Only	0.173	0.295	0.251	0.590	0.061
SD	0.162	0.279	0.235	0.583	0.285
SDR*	0.143	0.251	0.213	0.572	0.264
SR	0.196	0.230	0.281	0.604	0.333
SRR*	0.196	0.328	0.284	0.603	0.351
Hokkaido					
SAR-Only	0.445	0.616	0.549	0.736	0.092
SD	0.516	0.681	0.619	0.780	0.515
SDR*	0.502	0.668	0.606	0.769	0.499
SR	0.527	0.690	0.631	0.783	0.511
SRR*	0.535	0.697	0.637	0.789	0.510
Kumamoto					
SAR-Only	0.082	0.151	0.141	0.560	0.022
SD	0.080	0.148	0.138	0.559	0.119
SDR*	0.066	0.124	0.117	0.541	0.117
SR	0.101	0.183	0.175	0.568	0.156
SRR*	0.166	0.284	0.277	0.609	0.161

3.3 DEM Versus RRIM as Relief Data Sources

The comparison between DEM-based (SD, SDR) and RRIM-based (SR, SRR) configurations reveals consistent performance differences across the study areas. In general, models incorporating RRIM achieve higher F-scores and IoU values than those using DEM alone. For example, in the Hokkaido case study the RRIM-based configuration (SR) improves the F-score from 0.681 to 0.690 relative to the DEM-based configuration (SD), while the inclusion of rainfall further increases the performance to 0.697 under the SRR configuration. Similar trends are observed in the Kumamoto site, where the SRR configuration achieves the best performance among all tested models.

These results suggest that RRIM provides a more informative representation of terrain morphology than DEM when used as an auxiliary input for landslide detection. RRIM enhances micro-topographic features, such as ridges and slope discontinuities, which are commonly associated with landslide scars. By emphasizing these geomorphological structures, RRIM allows the segmentation model to better distinguish landslide areas from surrounding terrain.

In contrast, DEM provides only elevation information and may not sufficiently highlight subtle terrain structures related to slope failures. Although DEM still contributes useful contextual information, its representation of terrain morphology is less expressive than RRIM in complex mountainous environments. Consequently, the integration of RRIM with SAR imagery provides a more effective representation of landslide-related geomorphological patterns, resulting in improved segmentation performance across multiple study areas.

3.4 SAR-Only Baseline Versus Multi-Source Fusion

The SAR-only baseline provides a useful reference for evaluating the contribution of additional geospatial inputs. Across the three study areas, SAR-only segmentation generally achieves relatively high pixel-level accuracy but lower IoU and F-score values. This discrepancy arises because radar backscatter signals alone often provide limited separability between landslide and non-landslide areas, particularly in complex mountainous terrain where surface roughness, vegetation cover, and imaging geometry can produce similar scattering characteristics.

The integration of terrain information and rainfall data substantially improves model performance. Configurations incorporating DEM or RRIM provide additional contextual information related to slope morphology and terrain structure, enabling the model to better distinguish landslide features from surrounding landscapes. Rainfall information further contributes to improved detection by representing environmental conditions associated with landslide triggering events.

Across all three case studies, multi-source configurations consistently outperform the SAR-only baseline in terms of F-score, IoU, and Cohen’s Kappa. The most notable improvements are observed in the Hokkaido study area, where the SRR configuration increases the F-score from 0.616 to 0.697. Similar trends are observed in the Kyushu and Kumamoto sites, although the magnitude of improvement is smaller due to differences in landslide size and spatial distribution. These results demonstrate that integrating complementary geospatial information with SAR imagery enhances the robustness and reliability of automated landslide mapping.

3.5 Boundary and Structural Metrics

While pixel-level metrics such as IoU and F-score quantify overall segmentation accuracy, they do not fully capture the geometric quality of mapped landslide boundaries. For post-disaster applications, accurate delineation of landslide perimeters is equally important, as boundary errors can significantly affect hazard assessment and subsequent modelling tasks. Therefore, this study additionally evaluates segmentation performance using Boundary F1-score and Hausdorff distance.

Across all study areas, incorporating terrain information consistently improve boundary delineation compared with the SAR-only baseline. In the Kyushu site, the Boundary F1-score increases from 0.061 in the SAR-only configuration to 0.351 in the SRR configuration, while the Hausdorff distance decreases from approximately 204 m to 192 m, indicating improved boundary alignment. Similar trends are observed in Kumamoto, where the Boundary F1-score improves from 0.022 to 0.161 when RRIM and rainfall are incorporated.

In the Hokkaido case study, terrain inputs also enhance structural delineation, although the improvements in boundary metrics are more moderate due to the already strong performance of the SAR-only baseline. These results suggest that incorporating terrain information helps the model better capture the spatial extent and shape of landslide scars.

Overall, the improvements in Boundary F1-score and reductions in Hausdorff distance demonstrate that multi-source inputs enhance not only pixel-wise detection accuracy but also the geometric fidelity of landslide mapping. Such improvements are particularly valuable for operational disaster response and

https://doi.org/10.5194/isprs-annals-XI-3-2026-895-2026 | © Author(s) 2026. CC BY 4.0 License.

geohazard modelling, where accurate representation of landslide boundaries are critical for subsequent risk assessment and mitigation planning.

3.6 Statistical Robustness

The experimental results demonstrate consistent improvements across multiple evaluation metrics and experimental configurations. In all three study areas, models incorporating additional geospatial inputs generally outperform the SAR-only baseline in terms of IoU, F-score, Cohen's Kappa, and balanced accuracy. These improvements are observed across multiple modality combinations, indicating that the observed performance gains are systematic rather than incidental.

Although formal statistical significance tests such as paired t-tests or non-parametric alternatives were not applied in this study, the magnitude and consistency of the observed improvements suggest that the benefits of multi-source data integration are meaningful. In particular, the improvements are evident across multiple metrics and study areas, including cases with different terrain conditions and landslide characteristics.

Furthermore, the experiments were conducted using consistent training and evaluation protocols across all configurations, ensuring fair comparisons between models. The reproducibility of performance trends across multiple experimental setups provides additional confidence in the robustness of the proposed framework for automated landslide mapping.

3.7 Generality of the Model

The model's applicability to ALOS-2 data was examined to assess its cross-sensor generalizability using post-event L-band SAR imagery from the Kyushu, Hokkaido, and Kumamoto sites. The corresponding ALOS-2 datasets are summarized in Table 4, and the performance of the best-performing multimodal configuration (SRR*) is reported in Table 5.

Table 4. Post-Event ALOS-2 Datasets Used to Evaluate Cross-Sensor Generalizability of the Multimodal Model.

Disaster Location	Disaster occurrence	ALOS-2 imaging date: orbital direction
Kumamoto	16/04/2016	29/04/2016: A
Kyushu	05~06/07/2017	07/07/2017: D
Hokkaido	06/09/2018	06/09/2018: A

Table 5 Precision, Recall, and F1-score for ALOS-2 Test Tiles, Demonstrating the Model's (SRR*) Performance on L-band SAR Imagery.

Site name	Precision	Recall	F1-Score
Kyushu	0.548	0.061	0.111
Hokkaido	0.657	0.475	0.551
Kumamoto	0.077	0.048	0.059

The results indicate that the model exhibits partial cross-sensor generalization, but its performance varies substantially among the case studies. Among the three sites, Hokkaido shows the strongest transferability, achieving Precision = 0.657, Recall = 0.475, and F1-score = 0.551 on ALOS-2 imagery. This suggests that the geomorphological characteristics of the Hokkaido landslides remain sufficiently distinctive for the model to capture even under a different SAR sensor configuration. In contrast, Kyushu shows much lower recall and an F1-score of 0.111, while Kumamoto yields the weakest transfer performance with an F1-score of 0.059.

These results suggest that the proposed framework retains some ability to detect landslide features across different SAR imaging conditions, but that its generalizability is limited by cross-sensor differences in wavelength, backscatter characteristics, spatial resolution, and acquisition geometry. Because the model was primarily developed using COSMO-SkyMed X-band SAR data, performance degradation on ALOS-2 L-band imagery is expected. The stronger transferability observed in Hokkaido further indicates that cross-sensor performance is also influenced by site-specific factors such as landslide size, density, and geomorphological distinctiveness.

Overall, the ALOS-2 evaluation demonstrates the potential of the framework for cross-sensor application, but also highlights the need for additional strategies to improve sensor-independent performance. Future work should investigate domain adaptation, sensor-specific normalization, and multi-sensor training approaches to enhance the robustness of landslide detection across different SAR missions.

3.8 Practical Implications for Operational Landslide Mapping

A key distinguishing feature of this study is its reliance on post-disaster SAR imagery supplemented by publicly available ancillary geospatial datasets, including terrain representations (DEM and RRIM) and rainfall information. Unlike many landslide extraction approaches that depend on both pre- and post-event imagery for change detection, the proposed framework requires only post-event SAR observations. This reduces data requirements and acquisition time and eliminating the need to locate and pre-process suitable pre-disaster images with matching geometry, orbit, or acquisition mode.

Although high-resolution SAR data from constellations such as COSMO-SkyMed are not publicly available for routine research use, they are increasingly procured for emergency response by governments and disaster management agencies. The ancillary datasets used in this study, including DEM-derived terrain representations and rainfall observations, are publicly available and reproducible. As a result, the model architecture and processing pipeline can be transferred to other regions once post-event SAR imagery becomes available.

For emergency response agencies, this capability translates into faster product generation and broader applicability. High-resolution, pixel-level landslide inventories can be produced within a short time after a disaster without waiting for suitable pre-event SAR acquisitions. In addition, the improved boundary delineation achieved through multi-source integration enhances the reliability of downstream analyses such as hazard modelling, infrastructure impact assessment, and prioritization of recovery efforts.

https://doi.org/10.5194/isprs-annals-XI-3-2026-895-2026 | © Author(s) 2026. CC BY 4.0 License.

By combining post-event SAR imagery with readily accessible geospatial datasets, the proposed framework offers a scalable pathway for integrating deep learning–based landslide detection into operational hazard mapping systems. Such an approach could support national disaster management platforms as well as international emergency mapping services, enabling faster and more consistent delivery of landslide information to decision-makes worldwide.

4. Conclusion and Future Work

Rapid and reliable landslide mapping following disaster events is essential for emergency response, hazard assessment, and post-disaster recovery planning. While Synthetic Aperture Radar (SAR) imagery provides an effective all-weather observation capability, extracting landslides from SAR data alone remains challenging due to speckle noise, terrain-induced distortions, and the limited separability between landslide and non-landslide surfaces.

This study developed a UNet-based segmentation framework for landslide detection using a single post-event SAR acquisition supplemented by ancillary geospatial datasets. Experiments conducted across three major landslide-triggering events in Japan (Kyushu, Hokkaido, and Kumamoto) demonstrate that integrating terrain information and rainfall data with SAR imagery improves landslide detection performance compared with SAR-only inputs. Across the study areas, multimodal configurations consistently achieved higher F1-scores and IoU values than the SAR-only baseline, indicating that complementary geospatial information provides important contextual cues for identifying landslide features.

Among the evaluated terrain representations, Red Relief Image Maps (RRIM) consistently outperformed conventional Digital Elevation Models (DEM), suggesting that the enhanced representation of micro-topographic features improves the model’s ability to delineate landslide scars. Rainfall information further improved model performance in several configurations by providing environmental context associated with landslide-triggering conditions.

A key advantage of the proposed framework is its reliance on a single post-event SAR image combined with openly available ancillary datasets. This design reduces data dependencies and enables rapid generation of landslide inventories without requiring pre-disaster SAR acquisitions. Such a workflow is particularly suitable for operational disaster response scenarios where rapid mapping is required immediately after an event.

Future work will investigate improved multimodal fusion strategies, including transformer-based architectures and adaptive weighting of input modalities. Additional research on rainfall representation and cross-sensor generalization across different SAR missions will further enhance the robustness and operational applicability of the proposed framework for large-scale landslide monitoring.

Acknowledgements

Authors would like to acknowledge the financial support by Small/Startup Business Innovation Research (SBIR).

References

Barbera, E., 2014: COSMO-SkyMed polarimetric data for soil moisture retrieval: capability of SAR data for landslide monitoring.

Bovenga, F., Wasowski, J., Nitti, D. O., Nutricato, R., & Chiaradia, M. T., 2012: Using COSMO/SkyMed X-band and ENVISAT C-band SAR interferometry for landslides analysis. *Remote Sensing of Environment*, 119, 272-285.

Chiba, T., Kaneta, S. I., & Suzuki, Y., 2008: Red relief image map: new visualization method for three-dimensional data. *The international archives of the photogrammetry, remote sensing and spatial information sciences*, 37(B2), 1071-1076.

Dosovitskiy, A., Beyer, L., Kolesnikov, A., Weissenborn, D., Zhai, X., Unterthiner, T., Dehghani M., Minderer M., Heigold G., Gelly S., Uszkoreit J., Houlsby, N., 2020: An image is worth 16x16 words: Transformers for image recognition at scale. *arXiv preprint arXiv:2010.11929*.

Ghorbanzadeh, O., Blaschke, T., Gholamnia, K., Meena, S. R., Tiede, D., & Aryal, J., 2019: Evaluation of different machine learning methods and deep-learning convolutional neural networks for landslide detection. *Remote Sensing*, 11(2), 196.

Guzzetti, F., Mondini, A. C., Cardinali, M., Fiorucci, F., Santangelo, M., & Chang, K. T., 2012. Landslide inventory maps: New tools for an old problem. *Earth-Science Reviews*, 112(1-2), 42-66.

Hong, D., Gao, L., Yao, J., Zhang, B., Plaza, A., & Chanussot, J., 2020. Graph convolutional networks for hyperspectral image classification. *IEEE Transactions on Geoscience and Remote Sensing*, 59(7), 5966-5978.

Liu, P., Li, Z., Xu, Q., Wang, C., & Crippa, B., 2021. Automatic landslide detection from SAR intensity images using deep convolutional neural networks. *Remote Sensing*, 13(9), 1784. https://doi.org/10.3390/rs13091784.

Mondini, A. C., 2017. Measures of spatial autocorrelation changes in multitemporal SAR images for event landslides detection. *Remote Sensing*, *9*(6), 554.

Ronneberger, O., Fischer, P., & Brox, T., 2015, October. U-net: Convolutional networks for biomedical image segmentation. In *International Conference on Medical image computing and computer-assisted intervention* (pp. 234-241). Cham: Springer international publishing.

Zhao, F., Zhang, C., & Geng, B., 2024: Deep multimodal data fusion. *ACM computing surveys*, 56(9), 1-36.

This contribution has been peer-reviewed. The double-blind peer-review was conducted on the basis of the full paper.
https://doi.org/10.5194/isprs-annals-XI-3-2026-895-2026 |